ChemistrySelect

Research Article
doi.org/10.1002/slct.202201639

Chemistry Europe
European Chemical Societies Publishing

www.chemistryselect.org

Electro, Physical & Theoretical Chemistry

A DFT Study towards the Amide cis-trans Isomerization Process of the Myc-Max Inhibitor Mycro 3 and Its Photophysical Properties; Synthesis and NMR Studies of the trans-Conformation

Dimitrios Mamalis,[a, b, c] Angeliki Panagiotopoulou,[d] Elias A. Couladouros,[e] Demeter Tzeli,*[a, c] and Veroniki P. Vidali*[b]

Mycro 3 is a synthetic pyrazolo[1,5-*a*]pyrimidine amide with interesting bioactivity having exhibited promising results in *in vivo* studies against pancreatic cancer. Even though it is a known compound, no data concerning its conformations have been reported before. The aim of this work is to investigate the formation of its *trans*- and *cis*- isomers, the photophysical processes of the isomerization, and the solvent effect via a DFT study. We found that this isomerization is a thermodynamically favourable reaction, having a small barrier of 10.3 kcal/mol in DMSO. Additionally, the calculated ^{1}H and ^{13}C NMR spectra of the two isomers revealed measurable differences. Furthermore, the $S_0 \rightarrow S_1$ excitation was found in vis area at 413 nm (*trans*-isomer), while the $S_2 \rightarrow S_0$ and $S_1 \rightarrow S_0$ excitations are charge *trans*fer (CT) and partially CT state in near-infrared and vis spectra, showing that mycro 3 also has the potential to be used as a photosensitizer. Finally, its synthesis and its NMR analysis revealed a good agreement with the proposed *trans* conformation.

Introduction

MYC oncoprotein is present in most human cancers, highlighting its great significance as a target protein. Recent literature in cancer research has shown the potency of pyrazolo[1,5-*a*]pyrimidine analogues to inhibit the MYC oncoprotein by interfering with the MYC-MAX dimerization, thus leading to tumour shrinkage and cancer cell apoptosis.[1,2,3] Among the pyrazolo[1,5-*a*]pyrimidine inhibitors, mycro 3 (Scheme 1) is a leading compound, exhibiting high *in vitro* and *in vivo* potency. In particular, it has been tested and showed remarkable results in animal studies involving pancreatic cancer.[1,2]

Mycro 3 is a synthetic amide developed over the pyrazolo[1,5-*a*]pyrimidine substituted core. Dalinger et al.[4] have reported the synthesis of similar heterocyclic amides. However, no data have been reported concerning either the geometry of the amide bond or the existence of an isomer.

Generally, amidic moieties exist in two configurations, the *cis* and the *trans* (Scheme 1), about the C–N bond between the carbonyl carbon and the nitrogen, a partially double bond between carbonyl carbon and the nitrogen in the amide exist, which restricts free rotation around it. Amongst those two configurations, the general trend is that the *trans* isomers tend to be more stable than the corresponding *cis* ones since the largest substituents are more distant, thus minimizing the steric repulsion.[5] Although the *trans* configuration is more common in nature over 103 times than the *cis*, the equilibrium covers a great range of values in synthetic molecules since bulkier and chemically attractive groups can present more interactions related to flexibility and resonance.[6] In these cases, the product usually exists as a mixture of amide rotamers by NMR spectroscopy,[7,8] whereas after some time, only the *trans* isomer is detected[7] due to a *cis* to *trans* isomerization which is a thermodynamically favourable, and often a very rapid reaction,[7] having an energy barrier of up to 20 kcal/mol and thus leading to inconveniences in isolating only the less stable isomer.[7,9,10,11] It is often suggested that the thermodynamic ratio is the inverse of the kinetic. The biosynthetic ratios and the ratio of isomers depend on the solvent selections, temperature, and other conditions.[11,12,13,14,15] The selective synthesis of one isomer has been achieved by substitution of adjacent

[a] *D. Mamalis, Prof. D. Tzeli*
Laboratory of Physical Chemistry, Department of Chemistry, National and Kapodistrian University of Athens, Panepistimiopolis Zografou, Athens 157 71, Greece
E-mail: tzeli@chem.uoa.gr
dtzeli@eie.gr
[b] *D. Mamalis, Dr. V. P. Vidali*
Institute of Nanoscience and Nanotechnology,
National Center for Scientific Research "Demokritos",
Ag. Paraskevi 153 41,
Athens, Greece
E-mail: v.vidali@inn.demokritos.gr
[c] *D. Mamalis, Prof. D. Tzeli*
Theoretical and Physical Chemistry Institute, National Hellenic Research Foundation,
48 Vassileos Constantinou Ave., Athens 116 35, Greece
[d] *Dr. A. Panagiotopoulou*
Institute of Biosciences and Applications, National Center for Scientific Research "Demokritos", Ag. Paraskevi 153 41, Athens, Greece
[e] *Prof. E. A. Couladouros*
Agricultural University of Athens, Department of Food Science and Human Nutrition, Iera Odos 75, Athens 118 55, Greece

Supporting information for this article is available on the WWW under https://doi.org/10.1002/slct.202201639

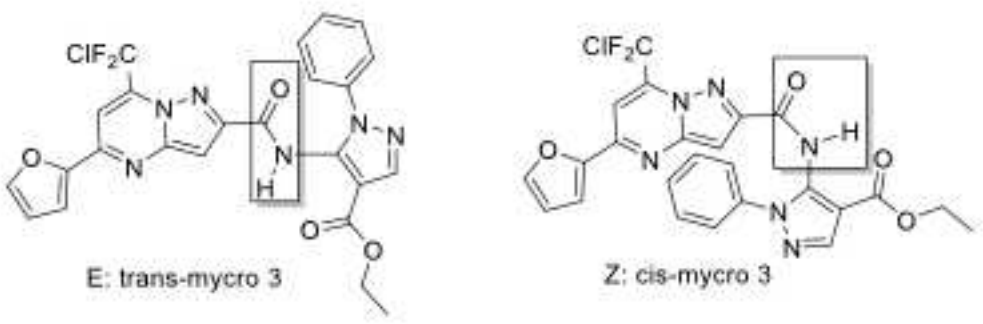

Scheme 1. *Trans* and *cis* isomers of mycro 3.

groups to restrict the rotation around the amide bond due to steric factors, which lead to a high-barrier conformational interconversion.[9,16] Note that the structure-based drug design typically utilizes only one conformation.

Generally, the binding of drugs to transport proteins and the interference of inhibitors to proteins are widely studied due to their importance in the pharmacological action of the drug in the organism. Furthermore, the interaction of these species with light may result in photosensitivity disorders. For this reason, extensive research efforts have been devoted to understanding the photosensitizing side effects of light on them.[17,18,19] Note that the existence of low-lying charge transfer states can influence their isomerization, their applications, or their inhibition properties.[20,21,22] Finally, molecules presenting absorption in particular excitation wavelengths can be used as photosensitizers and even they could be candidates as photosensitizers in photodynamic therapy (PDT).[21–23]

Mycro 3 presents an interesting bioactivity having exhibited promising results in *in vivo* studies against pancreatic cancer. Its analogues inhibit the MYC oncoprotein by interfering with the MYC-MAX dimerization,[1,23,24,25] highlighting the need for data regarding the geometry of minima energy structures for both *trans* and *cis* isomers of mycro 3, as well as their isomerization energy path. Since no data have been reported for the geometry of mycro 3 nor the existence of any isomers, herein, we wish to present the results of theoretical studies indicating the potential of formation of *cis* and *trans* conformations and *cis*→*trans* isomerization. NMR experiments to confirm the *trans* configuration of the isolated form of mycro 3 are shown, while calculations of ^{1}H and ^{13}C NMR spectra to verify measurable differences between the two isomers are also presented. Finally, the photophysical properties of the two isomers are studied to understand the photosensitizing side effects with light which could affect the isomerization via charge transfer states, indicating its potential use as a photosensitizer.

Results and Discussion

DFT calculations were carried out to obtain the lowest in energy *trans* and *cis* isomer of mycro 3 molecule. A series of *trans* and *cis* conformers which differ to the relevant position of two or more C–C and/or N–C rotation have been geometry optimized. Then for the obtained structures, the frequencies were calculated to confirm that they are true minima structures. In total, 5 *trans* and 11 *cis* conformers which are true minima, i.e., they have no imaginary frequency, were obtained. The B3LYP,[26] M06-2X,[27] PBE0,[28] and TPSSh[29] functionals were used in conjunction with the 6-31+G(d,p), 6-311+G(d,p) and 6-311+G(2d,p) basis sets.[30] Transition states between the lowest in energy *cis* and *trans* minimum structures were calculated, using the synchronous transit-guided quasi-Newton (STQN) method[31] and the potential energy curve with respect to the reaction coordinate, namely the ω(C10C11NC12) dihedral angle (see Scheme 2), was plotted.

The solvent effect was studied explicitly and implicitly. Three solvents were used, i.e., the dimethyl sulfoxide (DMSO), which is a highly polar organic reagent, the toluene (TOL), a non-polar solvent and dichloromethane (DCM), which is only slightly miscible with water, and it dissolves a huge variety of compounds. The polarizable continuum model (PCM)[32] model was used for the implicit insertion of the solvent. PCM model is divided into a solute part lying inside a cavity, surrounded by the solvent part represented as a structureless material characterized by its macroscopic properties, i.e., dielectric constants and solvent radius. This method reproduces solvent

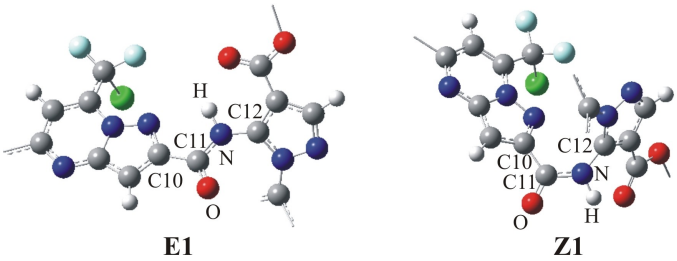

Scheme 2. Amide bond of **E1** and **Z1** global minima structures.

effects generally well.[33] The dielectric constants of the three solvents are ε = 46.826 (DMSO), 2.3741 (TOL), and 8.93 (DCM). Additionally, the solvent effect was induced explicitly with the addition of 6 (DMSO), 5 (TOL) and 5 (DCM) molecules via the ONIOM methodology.[34] In this methodology, the system was defined as two regions (layers) with the high layer, which is the mycro 3 molecule calculated at DFT level of theory, and the low layer, which is the solvent molecules calculated at the PM6[35] level of theory. Furthermore, the solvent effect on isomerization was studied simultaneously explicitly and implicitly. Finally, it should be noted that the main solvent that used in our computational part is the DMSO, because our experimental ^{1}H NMR and ^{13}C NMR spectra were recorded in DMSO-d6 solvent, with which distinct spectra are obtained. This solvent was also used by Dalinger et al.[4]

The IR, ^{1}H NMR, ^{13}C NMR, UV-vis absorption and emission spectra were calculated. NMR shielding tensors have been computed with the Gauge-Independent Atomic Orbital (GIAO) method.[36] The relative shifts have been estimated using the corresponding TMS shielding calculated in advance at the B3LYP/6-311 + G(2d,p) level of theory. The absorption and the emission spectra of the isomers were obtained via Time Dependent DFT (TD-DFT) calculations including 20 singlet-spin excited electronic states. The accuracy of the present methodologies has been confirmed by the fact that theoretical calculations using the functionals employing here can predict the vis-UV and IR spectra for amides and amines in very good agreement with experimental data.[37,38,39,40,41,42,43,44] All calculations were carried out using the Gaussian16 suite of codes.[45]

Geometry & Energetics: At first, a conformational analysis of mycro 3 was conducted in order to find the lowest in energy *trans* and *cis* isomers at the B3LYP/6-31 + G(d,p) level of theory in DMSO solvent. For all geometry optimized structures, their frequencies were calculated to clarify if they are minima or transition states. In total, we found 5 *trans* (**E**) and 11 *cis* (**Z**) minima structures, see Figure 1.

The calculated **E** structures lie within 2.49 kcal/mol and the Z structures are within 2.94 kcal/mol, see Figure 1. The lowest

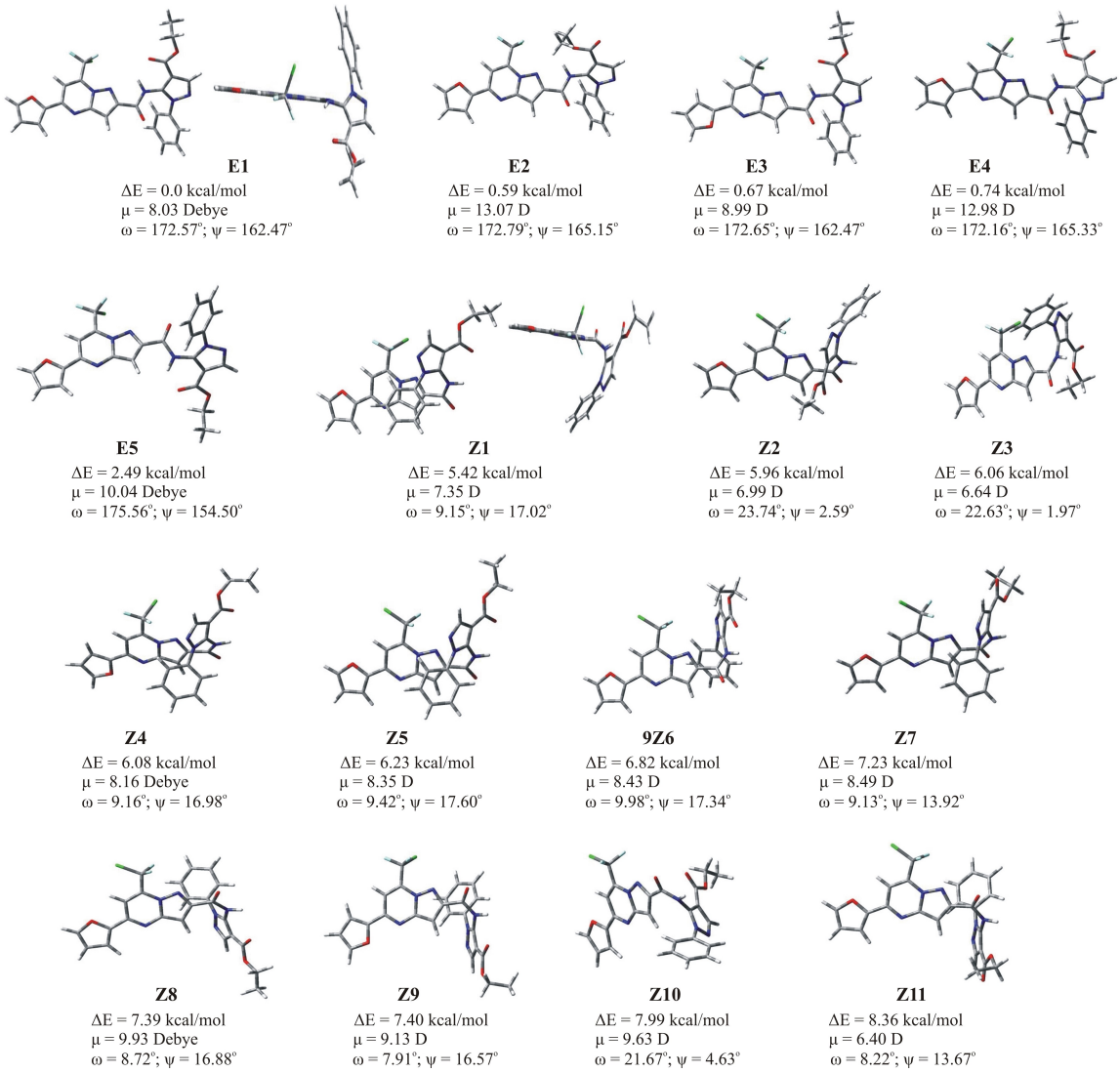

Figure 1. 5 *trans* (**E**) and 11 *cis* (**Z**) calculated minima structures of mycro 3.

in energy *trans* minimum structure isomer (**E1**) is lower in energy than **Z1** by only 5.42 kcal/mol, see Figure 1. The dipole moments of the calculated minima range from 6.40 to 13.07 Debye and their values reflect the relative positions of the groups in the mycro 3 compound. All five **E** isomers are rotamers, and so as the eleven **Z** isomers. Each **E** can be converted to another **E** isomer via one or more C–C rotations. For instance, the **E1** and **E2** rotamers differ in two C–C rotations in the ester group, their energy difference is 0.59 kcal/mol and the dipole moment is increased by 5 Debye in **E2**; while the **E1** and **E3** rotamers differ in a C–C rotation resulting to a rotation of the furan group, their energy difference is 0.67 kcal/mol and the dipole moment is less increased, i.e., by 1 Debye. In the calculated isomers we observed that van der Waals H bonds are formed as also π-π stacking interactions between the aromatic rings in order the minima structures to be stabilized. In **E1**, the amidic hydrogen (see Figure 2) forms two weak hydrogen bonds with the O atom of ester and the N atom of pyrazole groups; the corresponding bond distances H…O and H…N are 2.252 and 2.308 Å. In **Z1**, the H…O bond distance between the amidic hydrogen (H1, see Figure 2) and the O atom of the ester group is 2.516 Å, larger than in **E1**. Additionally, a π-π stacking interaction is formed between the pyrazolopyrimidine and the phenyl group; the distance between the centers of the groups is 4.31 Å, i.e., a typical distance of the π-π stacking interaction. Note that the π-π stacking distance between aromatic rings range from 3.5 to 4.5 Å,[46] while the stabilization energy of prototype benzene dimer is 2.5 kcal/mol at CCSD(T)/aug-cc-pVTZ level of theory.[47] The dihedral angles ω (C10C11NC12) and ψ (OC11NH) of the calculated minima structures of mycro 3 (Scheme 2) are given in Fig. 1. Due to steric factors, these angles are not 180 degrees in **E** isomers and 0 degrees in **Z** isomers. In **E** isomers, the deviation from these values ranges from 4.6 to 7.4 degrees for **ω** and from 14.7 to 25.5 for **ψ**. In **Z** isomers, the deviation from these values ranges from 7.9 to 23.7.4 degrees for **ω**, i.e., larger deviations than **Z** isomers, and from 2.0 to 17.3 for **ψ**. Note that, in **Z** isomers, large deviation at **ω** angles results in small deviation at **ψ** angles and vice versa.

Additional calculations for the lowest in energy **E** and **Z** minimum structure isomers using four functionals and three basis sets have been carried out, see Table 1. All levels of theory predict the same structure for the **E1** and **Z1** minima structures. The geometries are almost identical, and the most significant differences are observed in angles ω and ψ, see Table 1. Comparing the relative energy differences ΔE at B3LYP, PBE0 and TPSSh/6-311+G(d,p) levels, we observe that PBE0 predicts the lowest value of 4.33 kcal/mol while the

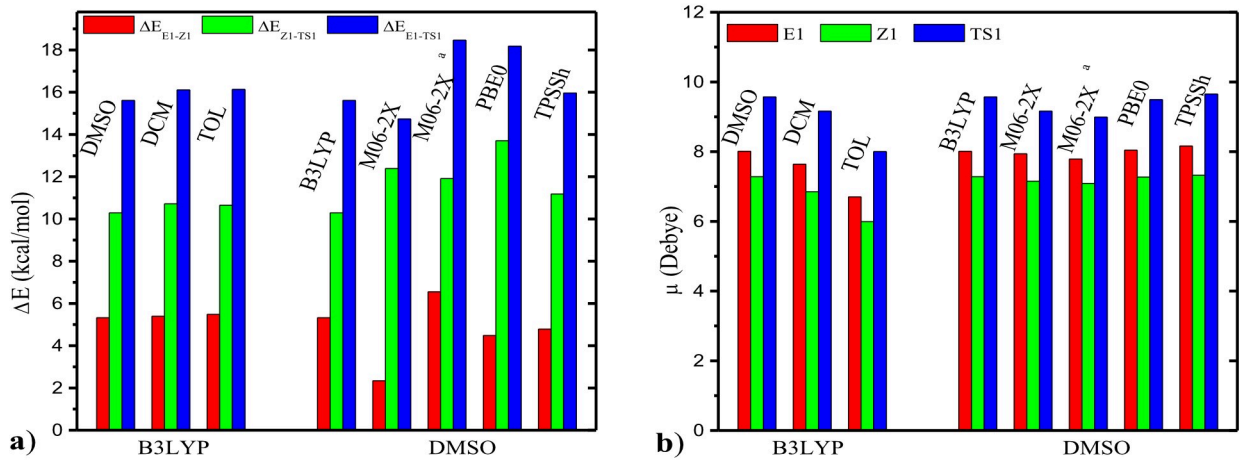

Figure 2. (**a**) Relative energy differences between **E1**, **Z1** and ΔE_{ZTS} between **Z1** and **TS1**. (**b**) Dipole moments μ of the **E1**, **Z1** and **TS1** structures of mycro 3 at different levels of theory, B3LYP. M06-2X, PBE0, and TPSSh/6-311+G(d,p). (M06-2X[a]: M06-2X/6-311+G(2d,p)).

Table 1. Dihedral angles ω(C10C11NC12) and ψ(OC11NH) of the **E1**, **Z1** and **9TS** structures of mycro3 at different levels of theory.

Methodology	Solvent	ω (degrees) E1	ψ (degrees)	ω (degrees) Z1	ψ (degrees)	ω (degrees) TS1[a]	ψ (degrees)
B3LYP/6-31+G(d,p)	DMSO	172.57	−162.47	9.15	17.02	74.62	116.38
B3LYP/6-31+G(d,p)	DCM	173.09	−161.58	9.26	19.38	74.39	117.84
B3LYP/6-31+G(d,p)	TOL	172.98	−160.48	9.56	22.90	76.16	120.09
M06-2X/6-311+G(d,p)	DMSO	170.57	−163.28	8.63	17.38		
PBE0/6-311+G(d,p)	DMSO	171.21	−162.64	9.67	18.27		
TPSSh/6-311+G(d,p)	DMSO	171.22	−162.21	10.02	18.71		

[a] At B3LYP/6-31+G(d,p), in DMSO solvent: **TS2** (ω=74.67 and ψ=116.14) and **TS3** (ω=73.87 and ψ=116.73).

B3LYP predicts the largest 5.32 kcal/mol, and TPSSh predicts a value of 4.33 kcal/mol, i.e., the values are similar. On the contrary, the M06-2X/6-311+G(d,p) method reverses the relative ordering of the **E1** and **Z1**, however when we add a 2d-type polarization basis set functions on all atoms but hydrogen, the ordering is corrected, and the **E1** becomes the lowest in energy minimum structure. Pictorially, the ΔE values in all used methodologies are plotted in Figure 2. Thus, we can conclude that B3LYP, PBE0 and TPSSh in conjunction with the 6-311+G(d,p) basis agree and are a good choice for the present study.

The dipole moments within the same solvent are similar for all four functionals. The choice of the solvent affects the dipole moment for both **E1** and **Z1** isomers (Figure 2). The largest values are observed for DMSO. DCM predicts values smaller than DMSO by about 0.4 Debye, while TOL predicts values smaller than DMSO by about 1.3 Debye. Note that the dielectric constants of the three solvents, which are a measure of their polarity, are $\varepsilon = 46.826$ (DMSO), 8.93 (DCM), and 2.3741 (TOL). We observe that the solvent with the largest ε value (a highly polar organic reagent) predicts the largest μ values, while the solvent with the smallest ε value predicts the smallest μ values, but the decrease of the μ is not proportional. This agrees with both experimental observation and mathematical analysis that dielectric constant of the solvent affects the measured value of the dipole moment.[48,49]

Isomerization: The *trans*ition state **TS1** between **E1** and **Z1** and two other *trans*ition states, i.e., **TS2** and **TS3**, are depicted in Figure 3. **TS1** and **TS2** differ in a C–C rotation resulting in a rotation of the furan group, their energy difference is 0.63 kcal/mol, while **TS1** and **TS3** differ in a C–C rotation resulting in a rotation of the CF_2Cl group, their energy difference is 0.68 kcal/mol. The ω and ψ angles range from 74.4 to 76.2 and 116.4 to 120.1 degrees in three used solvents. These angles differ from 90 and 180 degrees, respectively, due to steric effects. The dipole moment is about 1.5 Debye larger than the value of the **E**1 minimum in all solvents and all used methodologies. The H…O vdW bond of amidic H and O of the ester group is 2.024 Å, smaller by 0.2 and 0.5 Å than the corresponding values of **E1** (2.252 Å) and **Z1** (2.516 Å), respectively. The energy requirements for the *cis* to *trans* isomerization is calculated at 10.3(13.7)[11.2] kcal/mol at the B3LYP(PBE0)[TPSSh]/6-311+G(d,p) levels of theory in DMSO solvent, see Table 1 and Figure 2. In the DCM and TOL solvent, it increases up to 0.4 kcal/mol. On the other hand, the energy requirements for the *trans* to *cis* isomerization is calculated at 15.7(18.2)[16.0] kcal/mol at the B3LYP(PBE0)[TPSSh]/6-311+G(d,p) levels of theory in DMSO solvent. Finally, it is of interest that the energy barriers calculated via M06-2X depend on basis set selection, i.e., the M06-2X/6-311+G(d,p) predicts no barrier for the Z1→TS1, the M06-2X/6-311+G(d,p)//B3LYP/6-311+G(d,p) predicts a smaller energy barrier than the other functionals, while the inclusion of a second set for the non-hydrogen atoms, i.e., M06-2X/6-311+G(2d,p) predicts similar energy barrier with the other used functional, i.e., B3LYP, PBE0 and TPSSh.

The potential energy curve (PEC) of the *cis* to *trans* isomerization with respect to the reaction coordinate $\boldsymbol{\omega}$ is depicted in Figure 4. Two PECs are plotted. In the first one, as the ω values change from almost 0 degrees (**Z1** isomer) to almost 180 degrees (**E1** isomer), the structures are geometry optimized for each specific ω value (Figure 4, solid line). In the second one, the geometry of the **Z1** is retained and only the ω value changes from almost 0 degrees (**Z1** isomer) to 180 degrees (Figure 4, dot line). We observe that if we retain the geometry of the **Z1** and we change only the ω angle, the gap is 23.0 kcal/mol and it is located at about $\omega = 90$ degrees (dot line in Figure 4), while the geometry optimization of the structures for specific ω values (solid line in Figure 4) minimize the gap at 10.3 kcal/mol and the ω angle is 74.4 degrees due to steric effects.

Vibrational analysis: The IR spectra of **E1**, **Z1** and **TS1** are plotted in Figure 5. There are differences between the three spectra. In general, **E1** present larger IR intensities up to 13% than Z1 and up to 25% than **TS1**. In all three calculated **TS** *trans*ition states, the first mode has an imaginary frequency, and it corresponds to a vibration of the O and the H atoms of the amide bond so as the structure to be converted to the **E** isomer. The first vibration of **E1** (and in all calculated **E** isomers) corresponds to a twist between the two R groups of the amide bond, i.e., the C10, C11, N, C12, H and O atoms remain at the same position during the vibration, see Figure 6. The first vibration of **Z1** (and in all **Z** isomers) corresponds to a vibration that brings near the aromatic groups around the amide bond, i.e., the π-π stacking distance fluctuates. Finally, the last vibration with the largest frequency value corresponds to the N–H bond stretching of the amide. The corresponding values of frequency of **E1**, **Z1**, and **TS1** are 3517.7, 3568.8 and 3403.4 cm^{-1}. We observe that in **TS1**, there is a red shift of the

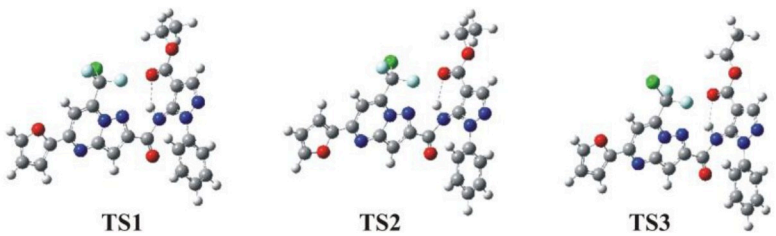

Figure 3. Three calculated *trans*ition states (**TS**) of mycro 3 at the B3LYP/6-31+G(d,p) level of theory in DMSO solvent.

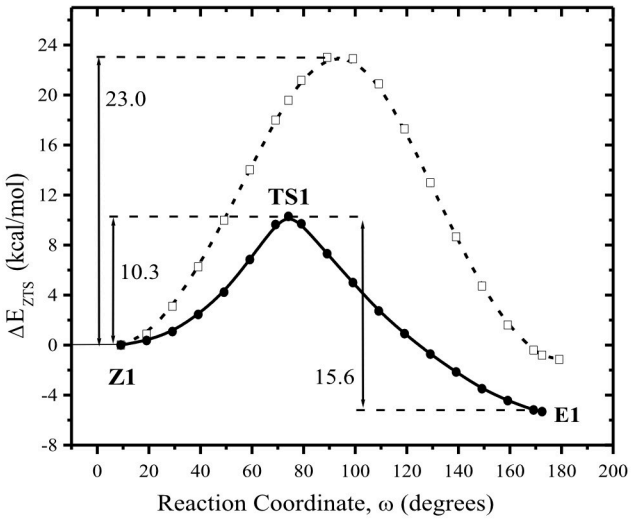

Figure 4. Potential Energy Curve of the *cis* to *trans* isomerization with respect to the reaction coordinate **ω**; i) optimized geometry structures for specific ω values (solid line) and ii) all distances, angles and dihedral angels but ω remain the same with those of **Z1** (dot line) at the B3LYP/6-311 + G(d,p) geometry level of theory in DMSO solvent.

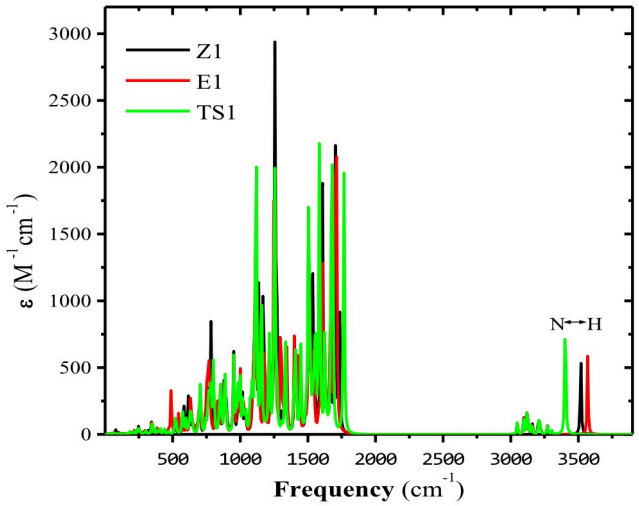

Figure 5. IR spectra of **E1**, **Z1** and **TS1** at the B3LYP/6-31 + G(d,p) level of theory in DMSO solvent.

N–H bond stretching of 114 and 165 cm^{-1} regarding **E1** and **Z1**, respectively. Thus, in **Z1**, where there is an intense steric effect, the bond stretching has the largest energy needs, while in **TS1**, where the N–H bond distance is largest, i.e., 1.025 (**TS1**), 1.019 (**E1**), and 1.016 (**Z1**), the bond stretching has the smallest energy needs. Finally, the IR intensity of N–H bond stretching is double in **TS1** than **Z1** and 75% than **E1**, see Figure 4.

Solvent Effect: To check the solvent effect, the solvent was induced explicitly and implicitly. Three solvents were used to reproduce the experimental conditions, i.e., the dimethyl sulfoxide (DMSO), which is a highly polar organic reagent, toluene (TOL), i.e., a non-polar solvent and dichloromethane (DCM), which is a commonly used solvent that dissolves a huge variety of compounds. The PCM model was used for the implicit insertion of the solvent. The solvent was induced explicitly with the addition of 6 (DMSO), 5 (TOL), and 5 (DCM) molecules via the ONIOM methodology so as interactions to be formed between the solvent molecules and mycro 3, see Figure 7. These van der Waals interactions affect the energy difference between **Z** and **E** isomers. We observe that the inclusion of the solvent only explicit induce an increase of the energy difference up to 0.5 kcal/mol compared to the implicit inclusion of the solvent, see Table 2. On the contrary, the

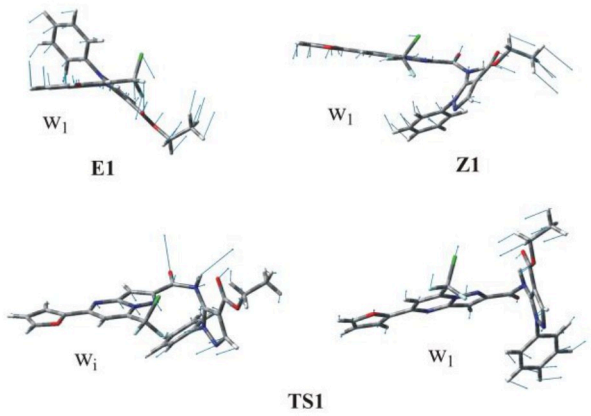

Figure 6. The lowest in energy frequency (w_1) of **E1**, **Z1** and **TS1** and the motion that corresponds to the isomerization (w_i) of **TS1** at the B3LYP/6-31 + G(d,p) level of theory in DMSO solvent.

energy difference between **E1** and **Z1** solvent is reduced when the solvent is included both implicitly and explicitly. Moreover, in DCM solvent, the reduction is significant, i.e., by 2 kcal/mol, which corresponds to a decrease by 40%.

UV-vis Spectra: The vertical excitation energies for the $S_0 \rightarrow S_x$ absorption and the emission maxima of the two lowest in energy excited states, their f-values, their main excitations, and corresponding coefficients for **E1**, **Z1**, and **TS1** in DMSO solvent as also electron density plots of the molecular orbitals (MO) involved in these excitations are collected in Table 3 and Figure 8. The absorption spectra are depicted in Figure 9. We observe that for both **Z** and **E** isomers, the $S_0 \rightarrow S_2$ excitation is a charge *transfer* (CT) excitation from R_8 to R_7, where R_8 is the group attached to C=O and R_7 is the group attached to NH. Thus, the R_8 group acts as electron donor and R_7 group acts as electron acceptor; while the maximum peak, i.e., $S_0 \rightarrow S_5$ excitation is a partially charge *trans*fer excitation and again R_7 accepts electron charge, see Figure 8. The first, second and fifth excitations are measured at 413 (vis), 344 and 318 nm. In the **TS1** structure both $S_0 \rightarrow S_1$ and $S_0 \rightarrow S_2$ excitations are partially CT. The H-1, H, L, and L + 1 MO of **E1** and **Z1** are similar, while the MO of **TS1** presents a difference only in H-1; moreover, energetically, the H-1 and H of **TS1** are nearly degenerate, see Figure 8. Additionally, the energy difference between H and L MO of the ground state of **E1** and **Z1** is decreased to half in the first excited state, see Fig. 8. The emission peak of the first excited state is a partially excited state within R_8, and it is located at about 1000 nm for **E1** and **Z1** and 723 nm for **TS1**, i.e., it is shifted by 280 nm at larger energy area, at red visible area. In the emission spectra of the second excited state, the excitation for **E1**, **Z1**, and **TS1** is a CT state, in **E1**, and **Z1** is

Table 2. Relative energy differences ΔE_{EZ} between **E1** and **Z1** of mycro 3 at the B3LYP/6-311 + G(d,p) level of theory including solvent explicitly and implicitly.

Solvent	ΔE_{EZ}(kcal/mol) Implicit	Explicit	Implicit + Explicit
DMSO	5.32	5.85	4.69
DCM	5.39	5.65	3.43
TOL	5.48	5.97	4.85

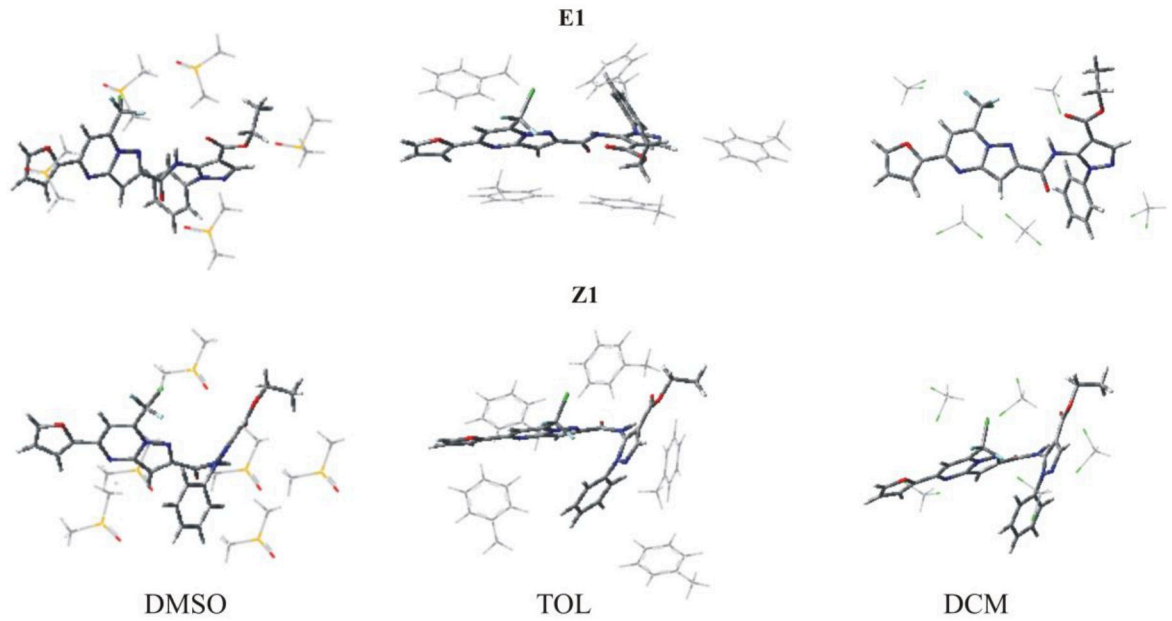

Figure 7. E1 and **Z1** isomers with the addition of 6 (DMSO), 5 (TOL) and 5 (DCM) molecules calculated at the B3LYP/6-311 + G(d,p) level of theory.

Table 3. Absorption and emission maxima, λ_{max}, vertical excitation energies ΔEv $S_0 \rightarrow S_x$ absorption maxima and vertical excitation energies ΔEv $S_\chi \rightarrow S_0$ emiision maxima, f-Values for absorption and emission, main excitations and their coefficients contributing to the excited state of **E1**, **Z1**, and **TS1** in DMSO solvent at the TD–B3LYP/6-311 + G(d,p) level of theory.

	ΔEv (eV) $S_0 \rightarrow S_1$	λ_{max} (nm)	f	coeff.	Excit.	ΔEv (eV) $S_1 \rightarrow S_0$	λ_{max} (nm)	f	coeff.	Excit.
E1	3.00	412.9	0.470	0.993	H→L	1.23	1006.7	0.065	1.000	H→L
Z1	3.01	411.9	0.408	0.993	H→L	1.24	996.6	0.061	1.000	H→L
TS1	2.83	437.7	0.015	0.702	H→L	1.72	722.6	0.003	0.973	H→L
				−0.649	H–1→L					
	$S_0 \rightarrow S_2$					$S_2 \rightarrow S_0$				
E1	3.61	343.7	0.143	0.863	H–1→L	1.88	658.0	0.016	−0.906	H–1→L
Z1	3.59	345.1	0.007	0.993	H–1→L	1.82	680.6	0.003	0.994	H–1→L
TS1	2.98	415.8	0.205	0.707	H–1→L	2.61	475.8	0.112	0.601	H–1→L
				0.684	H→L				0.773	H→L + 1
	$S_0 \rightarrow S_5$					$S_3 \rightarrow S_0$				
E1	3.89	318.5	0.681	0.891	H→L + 1					
Z1	3.93	315.6	0.658	0.936	H→L + 1					
TS1	3.77	328.7	0.550	−0.548	H→L + 1	2.62	473.0	0.138	−0.794	H–1→L
				0.666	H-2→L				0.585	H→L + 1

located at 658 and 681 nm in the red visible area while in **TS1** is located at 473 nm in the blue visible area.

Finally, it is interesting that the $S_2 \rightarrow S_0$ and $S_1 \rightarrow S_0$ excitations are charge *trans*fer (CT) and partially CT state in the near infrared and vis spectra area, i.e., above the high tissue absorption area of > 400 nm, showing that mycro 3 has the potential to be used as a photosensitizer.

The vertical and adiabatic excitation energies for the *trans*ition $S_0 \rightarrow S_1$ of **E1** and **Z1** are the same, i.e., 69 and 57 kcal/mol, respectively. For **TS1**, the corresponding values are smaller, i.e., 65 and 51 kcal/mol, respectively, see Table 4. In the first excited state, the ω and ψ dihedral angles of **E1** and **Z1** are similar to those of the ground state. On the contrary, in **TS1**, there are differences up to 30 degrees, i.e., ω = 95.6 and ψ = 84.0 in S_1 compared to ω = 74.6 and ψ = 116.4 in S_0; thus, the ω and ψ values in S_1 are nearer to 90 degrees than in S_0. Finally, it should be noted that on the potential energy surface of the first excited state, the energy gap for the **Z** to **E** isomerization is significantly smaller than in the ground state, i.e., a reduction of 64% compared to the gap of the ground state, 3.79 kcal/mol versus 10.3 kcal/mol.

NMR spectra: The calculated ^{1}H, ^{13}C NMR chemical shifts of **E1**, **E2**, **Z1**, and **TS1** have been calculated at the B3LYP/6-31 + G(d,p) level of theory in DMSO solvent and they are plotted in Figure 10 and Fig2S-3S of the SI and are given in Table 5 and Table 3S of SI. The amide H has a ^{1}H NMR shift of 10.793 ppm (**E1**), 10.092 ppm (**E2**), 8.533 ppm (**Z1**), and 9.476 ppm (**TS1**). Thus, the isomers can be clearly observed experimentally. **E1**

Table 5. Experimental[theoretical at B3LYP/6-311 + G(d,p)] ^{1}H & ^{13}C NMR chemical shifts (ppm) for mycro3a (*trans*) in DMSO-d_6, at 25 °C.

Atom Number	^{1}HNMR	Atom Number	^{13}CNMR
H–1	8.09[8.31]	C–1	147.45
H–2	6.84[7.29]	C–2	113.38
H–3	7.77[8.08]	C–3	115.58
H–4	–	C–4	150.24
H–5	–	C–5	137.33
H–6	8.01[8.31]	C–6	104.35
H–7	–	C–7	120.02
H–8	–	C–8	149.55
H–9	7.37[7.49]	C–9	98.41
H–10	–	C–10	147.39
H–11	–	C–11	160.46
H–12	–	C–12	137.96
H–13	–	C–13	110.20
H–14	8.22[8.50]	C–14	141.29
H–15	–	C–15	137.76
H–16 & H–20	7.64[7.92]	C–16 & C–20	123.83
H–17 & H–19	7.52[7.87]	C–17 & C–19	129.27
H–18	7.44[7.95]	C–18	128.48
H–21	–	C–21	161.50
H–22	4.18[4.29]	C–22	59.85
H–23	1.15[1.41]	C–23	14.01
H–24	–	C–24	124.64
NH	10.53[10.79]	–	–

Table 4. Vertical and adiabatic excitation energies ΔEv, ΔEa with respect to the ground state, relative energy differences ΔE_1 between the first excited states of **E1**, **Z1**, and **9TS1** and their dihedral angles ω, ψ and dipole moments μ at the TD–B3LYP/6-311 + G(d,p) level of theory in DMSO solvent.

	ΔEv($S_0 \rightarrow S_1$) (kcal/mol)	ΔEa($S_0 \rightarrow S_1$) (kcal/mol)	ΔE_1 (kcal/mol)	ω(S_1) (degrees)	ψ(S_1) (degrees)	μ(S_1) (debye)
E1	69.3	57.2	0.00	172.66	−162.87	10.92
Z1	69.4	57.3	5.44	8.92	17.13	11.85
TS1	65.3	50.8	9.22	95.64	83.97	11.49

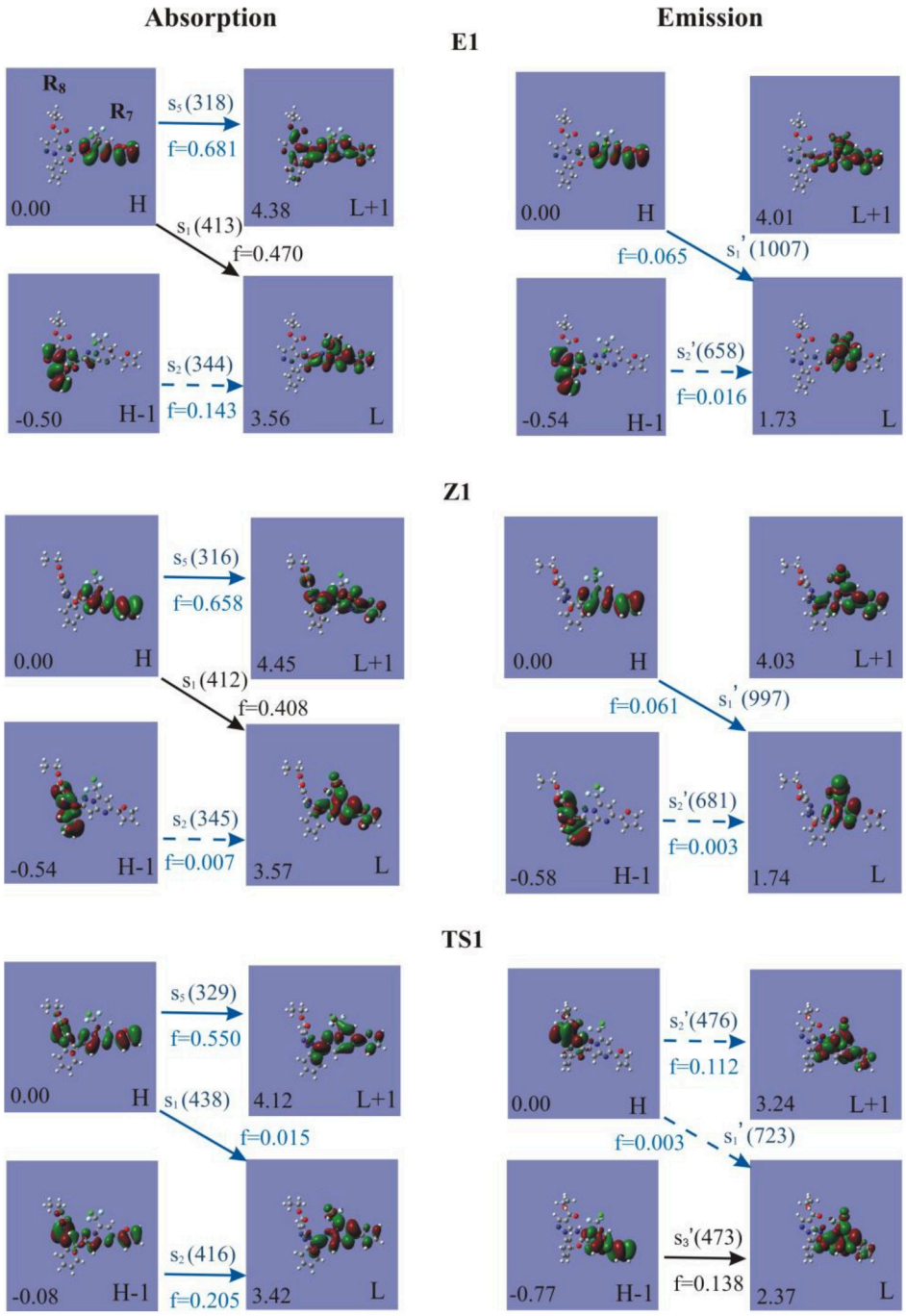

Figure 8. Electron density plots of the molecular orbitals involved in the absorption excitations corresponding to the major peaks for s_1 ($S_0 \rightarrow S_1$), s_2 ($S_0 \rightarrow S_2$), and s_5 ($S_0 \rightarrow S_5$) *trans*itions and in emission excitations s_1' ($S_1 \rightarrow S_0$), s_2' ($S_2 \rightarrow S_0$), and s_3' ($S_3 \rightarrow S_0$), of **E1**, **Z1**, and **TS1** in DMSO solvent. Relative energies of MO, f-values and λ_{max} in nm of the singlet (black solid arrows), CT excitations (blue dash arrows) and partially CT excitations (blue solid arrows) are given.

has the largest downfield shift. The amidic H is very highly deshielded due to fact that it is better surrounded by the carboxyl and the $-CF_2Cl$ groups. The difference between **E1** and **E2** is that the amidic H forms van der Waals bond with different O atoms, i.e., H…O=C in **E1** and H…O–C=O in **E2**. Thus, in **E1** is deshielded better. Regarding the ^{13}C NMR chemical shifts, the most downfield shift is observed for the C atom of the carboxylic group, of 152.26 ppm (**E1**), 150.52 ppm (**E2**), 154.51 ppm (**Z1**), and 158.38 ppm (**TS1**) and the largest one is observed in the **TS1**.

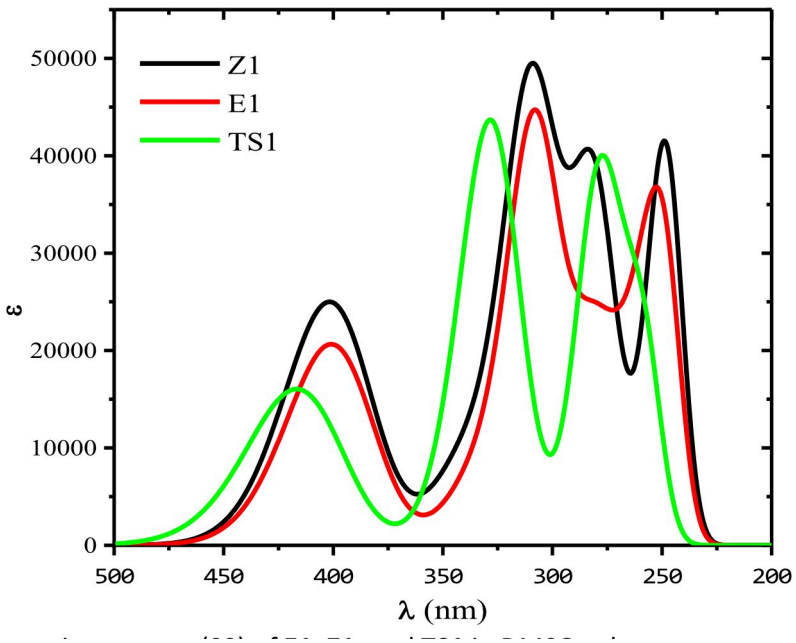

Figure 9. vis-UV Absorption spectra (S0) of **E1**, **Z1**, and **TS1** in DMSO solvent.

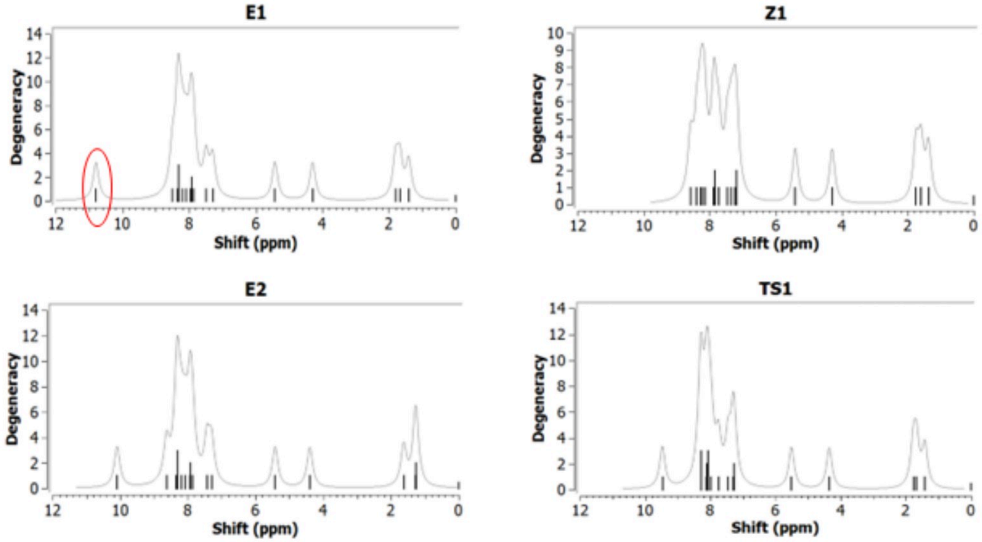

Figure 10. ^{1}H NMR spectra of **E1**, **E2**, **Z1**, and **TS1** at B3LYP/6-31+G(d,p) in DMSO solvent; reference compound: TMS, NMR degeneracy tolerance: 0.05, NMR peak half-width at half height: 0.01.

Synthesis and NMR studies of the isolated form of mycro 3

Synthesis and NMR experiments of mycro 3 were conducted to confirm its *trans*-geometry and to study its conformation. The synthetic route to mycro 3 was based on previously developed approaches,[4] for similar heterocycles modified appropriately (see Supporting Information)

The isolated form of mycro 3 was fully characterized by 1D and 2D NMR spectroscopy. NMR spectra of the isolated compound were obtained in DMSO-d6 and recorded on a Bruker Avance DRX-500 instrument at 25 °C. Assignment of ^{1}H and ^{13}C chemical shifts was based on ^{1}H-^{1}H correlations through bonding (COSY) and ^{1}H-^{13}C correlations from HSQC and HMBC spectra, whereas ^{1}H-^{1}H correlations through Rotating frame Overhause Effect (ROESY), were also studied. The main ^{1}H-^{1}H COSY, ^{1}H-^{1}H ROESY and ^{1}H-^{13}C HMBC correlations from 2D experiments are depicted in Figure 11.

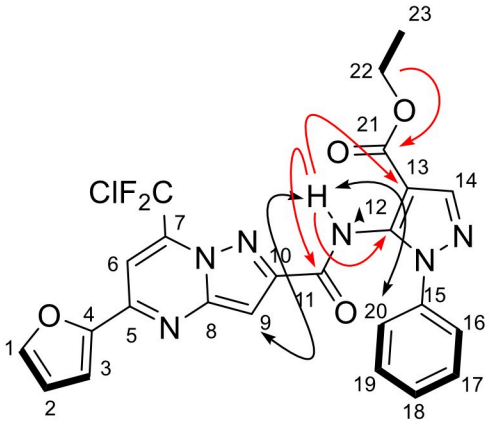

Figure 11. Selected ^{1}H-^{1}H COSY (bold bonds), ^{1}H-^{1}H ROESY (double arrows) and ^{1}H-^{13}C HMBC (red arrows) correlations for mycro 3.

The assignment of ^{1}H and ^{13}C NMR spectra as deduced by the NMR experiments is depicted in Table 5 (atom numbering shown in Figure 11 is followed). There is a very good agreement between calculated and experimentally measured ^{1}H NMR chemical shifts, see Table 5. The same trends are observed in both theoretical and experimental chemical shifts, the difference between the corresponding shifts ranges from 0.1 to 0.5 ppm and on the average the calculated chemical shifts are larger by about 3 % than the experimental ones.

The above assignment was supported by the 2D NMR experiments (see Supplementary material). Proton at 10.53 ppm – which corresponds to the NH proton- showed HMBC correlations with C-11 (160.46 ppm), C-12 (137.96 ppm) and C-13 (110.20 ppm). A long-range ^{1}H-^{13}C coupling between H-22 (4.18 ppm) and C-21 (161.50 ppm) was also detected to indicate the chemical shift of the carboxylic carbon.

Moreover, the chemical shift of the NH proton of the amide bond, observed at 10.53 ppm, is in very good agreement with the NH proton theoretically calculated for **E1** (10.79 ppm). Similarly, both the chemical shift of the H-23 and H-24 protons measured at 4.18 ppm and 1.15 nm are in good agreement with the calculated values of 4.29 and 1.41 ppm, respectively.

In addition, the ^{1}H-^{1}H ROESY experiment (Figure 12) demonstrated spatial proximity of the amide proton (NH, 10.53 ppm) to the H-16/H-20 protons (7.64 ppm) and the H-9 proton (7.37 ppm). These ROE signals indicate that the distances through space of the pairs NH–H16/H20, NH–H9 and NH–H22 in the experimental conformation of mycro 3 lies in the range of 2.5-5 Å. These results agree with our theoretical calculations and the **E1** model-built structure (Table 6).

Summary and Conclusions

Mycro 3 is a synthetic molecule that has been tested and has exhibited promising results in in vivo studies against pancreatic cancer. Up to now, only one isomer has been reported in the literature. In the present work, theoretical conformational analysis of the mycro 3 has been carried out to examine the possibility of the isomerization of the *trans* to *cis* isomer and vice versa. We analyzed how the choice of the solvent (highly polar organic reagent, non-polar solvent and slightly miscible with water solvent) can influence the isomerization. Finally, the photophysical properties of the two isomers has been examined to establish the relation and differences between the two isomers. We found that the *cis* to *trans* isomerization is a thermodynamically favourable reaction, having a relatively small energy barrier of 10.3 kcal/mol in DMSO. The solvent effect on the *cis* to *trans transformation* was studied explicitly and implicitly, and it was shown that it affects only slightly the isomerization barrier. Finally, the absorption and emission spectra of the isomers were calculated. The $S_0 \rightarrow S_1$ excitation is found in the vis area at 413 nm (E isomer). The $S_2 \rightarrow S_0$ and $S_1 \rightarrow S_0$ excitations are charge *trans*fer (CT) and partially CT state in vis and near infrared spectra, showing that mycro3 has the potential to be used as a photosensitizer. Furthermore, as far as we know, the calculated vis-UV and IR spectra are new

Table 6. Calculated distances through space of NH…H–16/H–20, NH…H–9 and NH…H–22.

		NH…..H–16/H–20	NH….H–9	NH….H–22
Theory:	E1	3.411	4.649	4.621
	E1-E7	3.221–3.482	2.431–4.653	3.414–5.926
Expt:	E	2.5–5	2.5–5	2.5–5

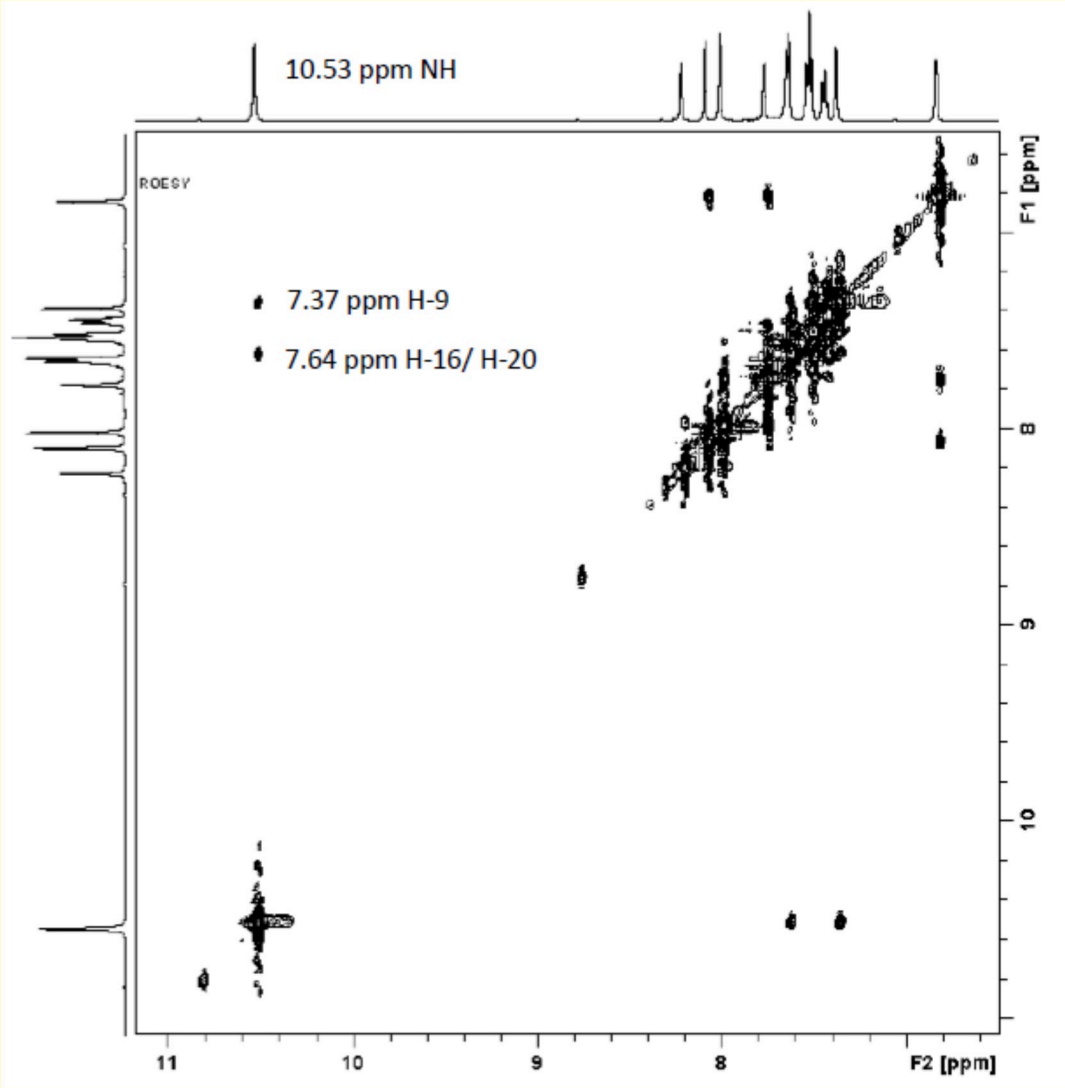

Figure 12. ^{1}H-^{1}H ROESYNMR spectrum of mycro3 in DMSO-d_6 at 25 °C (range δ_H 11.2–6.5). The numbering of the atoms is shown in Figure 11.

information, they show interesting properties of the compound, and they could be useful for whoever want to measure them experimentally. Also, synthesis and NMR experiments conducted for the isolated form of mycro 3 were in good agreement with theoretical calculations supporting the **E1** as the most stable conformation. Current efforts to establish the conditions of formation and isolation of the *cis*-isomer of mycro 3 (lower temperature, other solvents) and its NMR analysis for an unambiguous structure confirmation are underway.

Supporting Information Summary

Geometries, energetics, IR spectra, ^{1}H and ^{13}C NMR spectra, absorption spectra, computational and experimental details. Supplementary data to this article can be found online at https://doi.org/

Acknowledgements

Authors acknowledge Prof. A. A. Tsekouras (Laboratory of Physical Chemistry, Department of Chemistry, NKUA, Athens), and Dr. M. Zervou (Institute of Biology, Medicinal Chemistry & Biotechnology, NHRF, Athens) for valuable discussions. DT acknowledges the National and Kapodistrian University of Athens, Special Accounts for Research Grants for supporting of this research through the project "SONFM" (KE 17034). AP and VPV acknowledge financial support by the European Union and Greek national funds through the Operational Program Competitiveness, Entrepreneurship and Innovation, under the call RESEARCH – CREATE – INNOVATE (project code: T1EDK-03532)."

Conflict of Interest

The authors declare no conflict of interest.

Data Availability Statement

The data that support the findings of this study are available in the supplementary material of this article.

Keywords: Cis-trans isomerization · density functional calculations · inhibitor · mycro-3 · NMR spectroscopy · synthesis

[1] A. Kiessling, R. Wiesinger, B. Sperl, T. Berg, *ChemMedChem.* **2007**, *2*, 627–630.
[2] D. Stellas, M. Szabolcs, S. Koul, Z. Li, A. Polyzos, C. Anagnostopoulos, Z. Cournia, C. Tamvakopoulos, A. Klinakis, A. Efstratiadis, *JNCI J. Natl. Cancer Inst.* **2014**, *106*.
[3] A. J. Bonham, N. Wenta, L. M. Osslund, A. J. Prussin II, U. Vinkemeier, N. O. Reich, *Nucleic Acids Res.* **2013**, *41*, 754–763.
[4] I. L. Dalinger, I. A. Vatsade, S. A. Shevele, A. V. Ivachtchenko, *J. Comb. Chem.* **2005**, *7*, 236–245.
[5] H. E. Hallam, C. M. Jones, *J. Mol. Struct.* **1970**, *5*, 1–19.
[6] A. Siltari, R. Viitanen, S. Kukkurainen, H. Vapaatalo, J. Valjakka, *Biol.: Targets Ther.* **2014**, *8*, 59–65.
[7] P. Patorski, E. Wyrzykiewicz, G. Bartkowiak, *J. Spectrosc.* **2013**, *2013*, 197475.
[8] C. B. de Koning, W. A. L. van Otterlo, J. P. Michael, *Tetrahedron* **2003**, *59*, 8337–8345.
[9] R. A. Al-Horani, U. R. Desai, *Tetrahedron* **2012**, *68*, 2027–2040.
[10] H. A. Baldoni, G. N. Zamarbide, R. D. Enriz, E. A. Jauregui, Ö. Farkas, A. Perczel, S. J. Salpietro, I. G. Csizmadia, *J. Mol. Struct.* **2000**, *500*, 97–111.
[11] X. Hu, W. Zhang, I. Carmichael, A. S. Serianni, *J. Am. Chem. Soc.* **2010**, *132*, 4641–4652.
[12] S. Deng, J. Taunton, *J. Am. Chem. Soc.* **2002**, *124*, 916–917.
[13] R. R. Gardner, S. L. McKay, S. H. Gellman *Org. Lett.* **2000**, *2*, 2335–2338.
[14] J. S. Laursen, J. Engel-Andreasen, P. Fristrup, P. Harris, C. A. Olsen, *J. Am. Chem. Soc.* **2013**, *135*, 2835–2844.
[15] K. N. Kirschner, R. J. Woods, *PNAS* **2001**, *98*, 10541–10545.
[16] S. Thakkar, J. S. M. Svendsen, R. A. Engh, *Molecules* **2018**, *23*, 2455.
[17] A. F. Monteiro, M. Rato, C. Martins, *Clin. Dermatol.* **2016**, *34*, 571–581.
[18] O. Molins-Molina, R. Perez-Ruiz, E. Lence, C. Gonzalez-Bello, M. A. Miranda, M. C. Jimenez, *Front. Pharmacol.* **2019**, *10*, 1028.
[19] I. Vayá, I. Andreu, E. Lence, C. González-Bello, M. C. Cuquerella, M. Navarrete-Miguel, D. Roca-Sanjuán, M. A. Miranda, *Chem. Eur. J.* **2020**, *26*, 15922–15930.
[20] K. Krukiewicz, J. K. Zak, *Mater. Sci. Eng. C* **2016**, *62*, 927–942.
[21] P. Agostinis, K. Berg, K. A. Cengel, T. H. Foster, A. W. Girotti, S. O. Gollnick, S. M. Hahn, M. R. Hamblin, A. Juzeniene, D. Kessel, M. Korbelik, J. Moan, P. Mroz, D. Nowis, J. Piette, B. C. Wilson, J. Golab, *Ca-Cancer J. Clin.* **2011**, *61*, 250–281.
[22] N. Holzmann, L. Bernasconi, R. H. Bisby, A. W. Parker, *Phys. Chem. Chem. Phys.* **2018**, *20*, 27778–27790.
[23] H. D. Arndt, *Angew. Chem.* **2006**, *118*, 4664–4673; *Angew. Chem. Int. Ed.* **2006**, *45*, 4552–4560.
[24] H. Mo, M. Henriksson, *Proc. Natl. Acad. Sci. USA* **2006**, *103*, 6344–6349.
[25] H. Mo, M. Vita, M. Crespin, M. Henriksson, *Cell Cycle* **2006**, *5*, 2191–2194.
[26] a) D. Becke, *J. Chem. Phys.* **1993**, *98* 1372; b) C. Lee, W. Yang, R. G. Parr, *Phys. Rev. B.* **1988**, *37*, 785–789.
[27] Y. Zhao, D. G. Truhlar, *Theor. Chem. Acc.* **2008**, *120*, 215–41.
[28] a) J. P. Perdew, K. Burke, M. Ernzerhof, *Phys. Rev. Lett.* **1996**, *77*, 3865–3868; b) M. Enzerhof, G. E. Scuseria, *J. Chem. Phys.* **1999**, *110*, 5029–5036; c) C. Adamo, V. Barone, *J. Chem. Phys.* **1999**, *110*, 6158–6170.
[29] J. M. Tao, J. P. Perdew, V. N. Staroverov, G. E. Scuseria, *Phys. Rev. Lett.* **2003**, *91*, 146401.
[30] L. A. Curtiss, M. P. McGrath, J.-P. Blaudeau, N. E. Davis, R. C. Binning Jr., L. Radom, *J. Chem. Phys.* **1995**, *103*, 6104–6113.
[31] C. Peng, P. Y. Ayala, H. B. Schlegel, M. J. Frisch, *J. Comput. Chem.* **1996**, *17*, 49–56.
[32] M. Cozi, G. Scalmani, N. Rega, V. Barone, *J. Chem. Phys.* **2002**, *117*, 43–54.
[33] a) J. Tomasi, B. Mennucci, R. Cammi, *Chem. Rev.* **2005**, *105*, 2999–3093; b) A. Pedone, J. Bloino, S. Monti, G. Prampolini, V. Barone, *Phys. Chem. Chem. Phys.* **2010**, *12*, 1000–1006.
[34] S. Dapprich, I. Komáromi, K. S. Byun, K. Morokuma, M. J. Frisch, *J. Mol. Struct.* **1999**, *462*, 1–21; T. Vreven, K. Morokuma, Ö. Farkas, H. B. Schlegel, M. J. Frisch, *J. Comb. Chem.* **2003**, *24*, 760–769; T. Vreven, K. Morokuma, *Annual Reports in Comp. Chem.* **2006**, *2*, 35–50.
[35] J. J. P. Stewart, *J. Mol. Model.* **2007**, *13*, 1173–213.
[36] a) F. London, *J. Phys. Radium* **1937**, *8*, 397–409;b) J. R. Cheeseman, G. M. Trucks, T. A. Keith, M. J. Frisch, *J. Chem. Phys.* **1996**, *104*, 5497–509.
[37] H. G. Bohr, K. J. Jalkanen, M. Elstner, K. Frimand, S. Suhai, *Chem. Phys.* **1999**, *246*, 13–36.
[38] V. Librando, A. Alparone, *Polycyclic Aromat. Compd.* **2007**, *27*, 65–94.
[39] D. Tzeli, T. Mercouris, G. Theorodakopoulos, I. D. Petsalakis, *Comp. Theor. Chem.* **2017**, *1115*, 197–207.
[40] D. Tzeli, I. Petsalakis, G. Theodorakopoulos, *Int. J. Quantum Chem.* **2019**, *119*, e25958.
[41] S. S.Meenakshi Sundaram, S. Karthick, K. Sailaja, R. Karkuzhali, G. Gopu, *J. Photochem. Photobiol. B* **2020**, *203*, 111735.
[42] D. Tzeli, I. D. Petsalakis, G. Theodorakopoulos, *Int. J. Quantum Chem.* **2020**, *120*.
[43] S. J. Porobić, B. Đ. Božić, M. D. Dramićanin, V. Vitnik, Ž. Vitnik, M. Marinović-Cincović, D. Ž. Mijin, *Dyes Pigm.* **2020**, *175*, 108139.
[44] C. E. Tzeliou, D. Tzeli, *J. Chem. Inf. Model.* **2022**, DOI: 10.1021/acs.jcim.2c00257.
[45] Gaussian 16, Revision A.03, M. J. Frisch, G. W. Trucks, H. B. Schlegel, G. E. Scuseria, M. A. Robb, J. R. Cheeseman, G. Scalmani, V. Barone, G. A. Petersson, H. Nakatsuji, X. Li, M. Caricato, A. V. Marenich, J. Bloino, B. G. Janesko, R. Gomperts, B. Mennucci, H. P. Hratchian, J. V. Ortiz, A. F. Izmaylov, J. L. Sonnenberg, D. Williams-Young, F. Ding, F. Lipparini, F. Egidi, J. Goings, B. Peng, A. Petrone, T. Henderson, D. Ranasinghe, V. G. Zakrzewski, J. Gao, N. Rega, G. Zheng, W. Liang, M. Hada, M. Ehara, K. Toyota, R. Fukuda, J. Hasegawa, M. Ishida, T. Nakajima, Y. Honda, O. Kitao, H. Nakai, T. Vreven, K. Throssell, J. A. Montgomery, Jr., J. E. Peralta, F. Ogliaro, M. J. Bearpark, J. J. Heyd, E. N. Brothers, K. N. Kudin, V. N. Staroverov, T. A. Keith, R. Kobayashi, J. Normand, K. Raghavachari, A. P. Rendell, J. C. Burant, S. S. Iyengar, J. Tomasi, M. Cossi, J. M. Millam, M. Klene, C. Adamo, R. Cammi, J. W. Ochterski, R. L. Martin, K. Morokuma, O. Farkas, J. B. Foresman, D. J. Fox, Gaussian, Inc., Wallingford CT, **2016**.
[46] D. Tzeli, I. D. Petsalakis, G. Theodorakopoulos, *Phys. Chem. Chem. Phys.* **2011**, *13*, 11965–11975.
[47] T. Janowski, P. Pulay, *Chem. Phys. Lett.* **2007**, *447*, 27–32.
[48] F. C. Frank, *Proc. Royal Soc. London. Series A, Mathematical and Physical Sciences* **1935**, *152*, 171–196.
[49] I. G. Ross, R. A. Sack, *Proc. Phys. Soc. B* **1950**, *63*, 893–906.

Submitted: April 24, 2022
Accepted: June 15, 2022